Supporting Information for:

Contrasting interchain order and mixed ionic-electronic conduction in conjugated polymers: an isoindigo case study

Rebecca F. Meacham,[a] Heejung Roh,[a] Camille E. Cunin,[a] Eric R. Lee,[a] Wenhao Li,[c] Yan Zhao,[c] Sanket Samal,[a,b,] Aristide Gumyusenge[a,*]*

[a]Massachusetts Institute of Technology, Department of Materials Science & Engineering, 77 Massachusetts Ave, Cambridge, MA, 02139, USA

[b]Purdue University, James Tarpo Jr. and Margaret Tarpo Department of Chemistry, 560 Oval Drive, West Lafayette, IN, 47907, USA

[c]Fudan University, Laboratory of Molecular Materials and Devices, State Key Laboratory of Molecular Engineering of Polymers, Department of Materials Science, Shanghai, 200438, China

Table of Contents

1. Materials and Experimental Methods....3

2. Monomer Synthesis....5

Scheme S1. Reaction conditions....5

3. Polymer Synthesis....9

Scheme S2. Polymerization Conditions....9

4. Molecular Weight determination....12

Table S1. Polymer molecular weight obtained from HT-GPC....12

Table S2. DOSY parameters and estimated molecular weights....13

5. Material Characterization....13

Figure S1. Thermal characterization of ***m*g-IID** polymers: A) TGA and B) DSC thermograms of the IID series.....13

Figure S2. UV-vis absorbance of ***m*g-IID** polymers in chloroform....14

6. Computational Simulations of HOMO and LUMO....14

Figure S3. DFT simulations of HOMO (A-C) and LUMO (D-F) for **0g** (top), **50g** (middle), and **100g** (bottom).....14

7. AFM....15

Figure S4. AFM height images of ***m*g-IID** films....15

8. Contact Angle and Surface Energy....15

Figure S5. Contact angle and surface energy measurements of ***m*g-IID** films....15

9. GIWAXs Parameters....15

Table S3. GIWAXs spacing parameters....15

10. DFT Configurations....16

Figure S6. Density functional theory (DFT) calculations of polymer backbones. The yellow and green lines are added for visualization of chain planarity....16

11. Electrochemical Performance....17

Figure S7. Cyclic voltammetry up to 100 cycles in 0.1M $LiPF_6$....17

Figure S8. Normalized spectro-electrochemical spectra of ***m*g-IID** thin films with increasing amounts of glycol sidechains....17

12. Electrochemical Impedance Spectroscopy....18

Figure S9. Bode plot of ***m*g-IID** series in 0.1M $LiPF_6$ at -0.6V with equivalent circuit for data fitting and equation for calculating ionic conductivity....18

13. OECT Performance....18

Figure S10. Characteristic transfer curves from ***m*g-IID** polymers in 0.1M $LiPF_6$ as the electrolyte....18

Table S3. μC* of ***m*g-IID** polymers....18

1. Materials and Experimental Methods

All starting materials were purchased from commercial sources and used without further purification. All reactions were carried out using air-sensitive synthesis methods and conditions adapted from the literature. ^{1}H NMR spectra were recorded using Bruker Avance-III HD Nanobay at 400MHz and Bruker Avance Neo at 500MHz and analyzed using Bruker Topspin and MestraNova software. Molecular weight and polydispersity data were collected on a TOSOH Bioscience EcoSEC HLC-8321 using 1,2,4-tricholorbenzene (TCB) at 150°C as the mobile phase at a flow rate of 1.0mL/min. Average molecular weight was determined using ^{1}H NMR Diffusion-Order Spectroscopy (DOSY) in $CDCl_3$ at ambient temperature. Differential scanning calorimetry (DSC) was measured with a TA Instruments DSC 2500 with a scan rate of 10°C/min. Thermal gravimetric analysis (TGA) was carried out on a TA Instruments Discovery 550 TGA with a scan rate of 10°C/min. UV-vis-NIR absorbance was measured using a Perkin Elmer 1050 UV-vis-NIR Spectrophotometer. Atomic force microscopy (AFM) images were obtained on a Bruker Dimension Icon XR SPM and processed with Gwyddion Software. Contact angle and surface energy were evaluated on a Rame-Hart Contact Angle Apparatus with DROPimage software.

Experimental energy level measurement

The electronic band structures were collectively constructed using the following measurements: X-ray Photoelectron Spectroscopy (XPS) with a monochromatic Al Kα source (1486.6 eV) and a -10 V bias applied. These measurements were conducted to obtain both the secondary electron cut-off and Fermi edge spectra for each sample. A gentle ion gun treatment (Monatomic source gun with 2000 eV, 30 seconds etch time) was performed to clean the surface. Tauc plots were converted from UV-vis-NIR spectra.

Standard metal (e.g., Au) is used to automatically calibrate the XPS binding energy scale. After calibrating the spectra, the value corresponding to 0 eV Fermi energy along the x-axis (Fermi region) is identified by extracting the point where the second derivative of the spectrum becomes zero. Then, the work function is obtained by subtracting the cut-off position from the photon energy following the equation:

$$\phi = h\nu - E_{cut-off}$$

where *hv* is the photon energy used in the XPS experiment, and the $E_{cut\text{-}off}$ is the binding energy at the secondary electron cut-off.

Electrochemical Characterization

CV measurements were carried out using a conventional three-electrode setup with 4.5 cm wide electrochemical cell to contain the liquid electrolytes during the measurements. Polymer film was coated onto ITO to serve as a working electrode and a spiral Pt wire was used as a counter electrode, versus an Ag/Ag+ reference electrode. The spectroelectrochemical absorption responses were then collected using a Perkin Elmer 1050 UV–vis-NIR spectrophotometer in combination with SP-300 Potentiostat (Biologic), using a cuvette to incorporate the same three-electrode setup. Electrochemical impedance spectroscopy was carried out in the same setup as CV measurements at -0.6V.

Grazing Incidence X-Ray Diffraction (GI-XRD)

The SiO2/Si wafers with 300 nm thermally grown SiO2 were used as substrates. The substrates were modified with OTS-self-assembled monolayer. Conjugated polymer solutions at a concentration of 8 mg/mL were spin-coated in ambient conditions at a spin speed of 1000 rpm for 60 seconds to form the semiconductor layers. Subsequently, the samples were annealed in a vacuum oven at 180°C for 20 minutes and then cooled down to room temperature. GI-XRD measurements were carried out at the BL15U beamline of Shanghai Synchrotron Radiation Facility (SSRF). An incidence angle of 0.10° and measurement time of 20 seconds was used with a beam energy of 10 keV. The distance between sample and detector as well as the scattering vector was calibrated by lanthanum hexaborate. Data from the GI-XRD patterns were analyzed using Dioptas 2.5.2 software.

Computational Simulations

All density functional theory (DFT) calculations were performed on the software package Gaussian 16.[1] The polymer chains were optimized at the B3LYP[2,3]/6-31G(d)[4] level of theory. The optimized structure confirmed their local minima by studying their frequency analysis and considering their zero-point vibrational energy during calculations.

The initial topology files for the polymer chains were obtained from Automated Topology Builder (ATB) and Repository (Version 3.0).[5] A force field based on GROMOS_54A7 was employed in molecular dynamics (MD) simulations. All MD simulations were performed with Lammps 29Oct20.[6] A large supercell consisting of 12 – 16 polymer chains was constructed using Moltemplate.[7] As an initial guess, the lamellar distance and π-π distances of large supercells were increased to 50 Å (40 Å for glycol chains) and 5 Å, respectively. At first, the chains were relaxed at 300 K (NVE ensemble, T = 300 K, dynamic time = 0.5 ns). Then, the chains were first heated to 375 K (NVT ensemble, T = 375 K, dynamic time = 0.5 ns) and cooled back to 300 K slowly at 1 atm (NPT ensemble, 1 atm, T = 375 – 300 K, dynamic time = 1 ns), to relax the lamellar distances and π-π stacking. After the thermalization process, the chains were further relaxed at 300 K and 1 atm (NPT ensemble, 1 atm, T = 300 K, dynamic time = 2 ns), and snapshots were taken at every 500 ps.

Device Fabrication and Measurement

OECT devices with dimensions of L=5µm and W=400µm were fabricated in the cleanroom environment. Source and drain electrodes were defined using photolithography with AZnLOF2020 photoresist and a mask-less aligner (Heidelberg MLA 150). A 10nm layer of Ti followed by a 100nm layer of Au was deposited using an e-beam evaporator (Temescal FC2000). Subsequently, a first layer of parylene-C was deposited using a Specialty Coating Systems PDS 2010, employing Silane A 174 (procured from Sigma Aldrich) as an adhesion promoter. A sacrificial layer of soap was spin-coated onto the wafer before applying a second layer of parylene-C. The channel and electrode pads were then defined using the same mask-less aligner

with AZ10XT photoresist and a reactive ion etching process (SAMCO 230iP). Channels were formed by spin-coating 5mg/mL solutions of polymers onto the devices at 2000rpm for 35 seconds via dynamic spin-coating. Following a peel-off step, the devices were baked inside a glovebox at 120°C for 30 minutes and allowed to cool for at least 1 hour before characterization. A PDMS sheet was cut to form a well and used to contain the electrolyte. Output and transfer characteristics of the OECT devices were then measured with an Ag/AgCl pellet as the gate using a Keithley 4200A and analyzed using OriginLab software.

2. Monomer Synthesis

Side chains and monomers were synthesized using modified procedures from literature.[8–16]

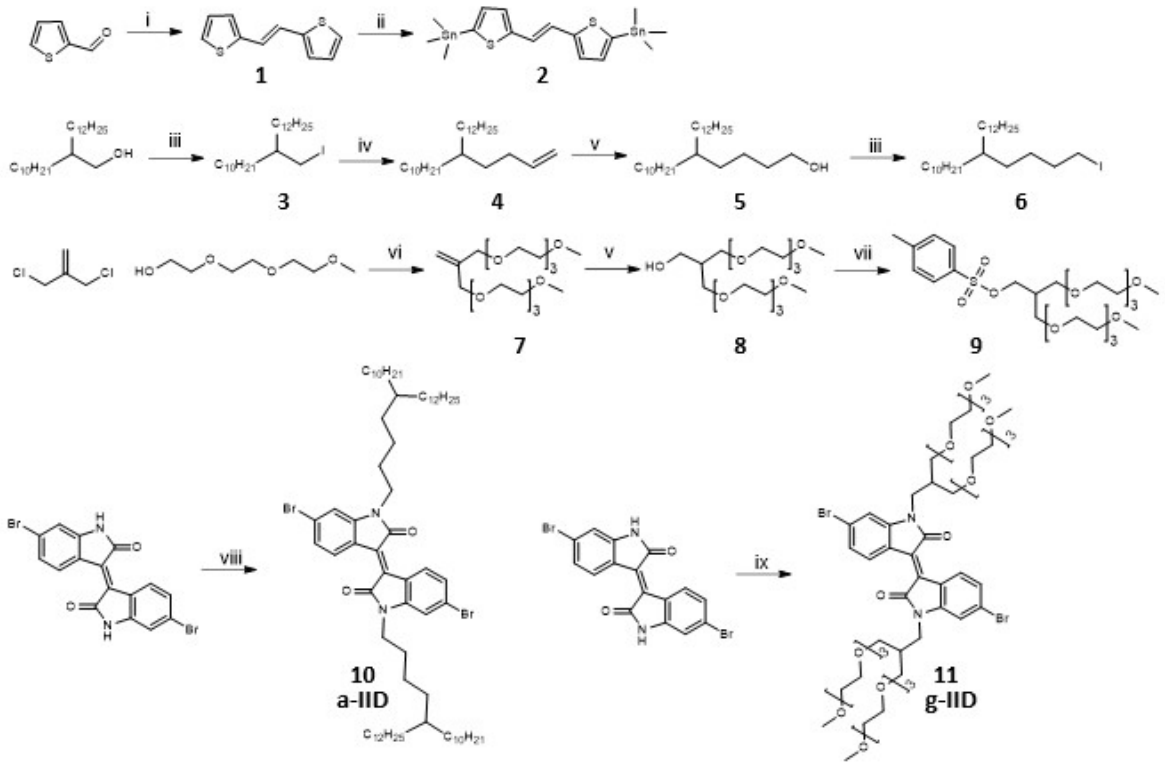

Scheme S1. Reaction conditions i) TiCl4, Zn, THF, -10°C; ii) nBuLi, Me3SnCl, THF, -78°C; iii) PPh3, I2, DCM, 0°C-RT; iv) 2M allyl magnesium chloride solution, THF, reflux; v) 9BBN, THF, H2O2, NaOH; vi) NaH, THF, 0°C; vii) TosCl, water, THF, 0°C-RT; viii) **6**, K2CO3, DMF, 110°C; ix) **9**, K_2CO_3, TBAB, DMF, 120°C.

2 was synthesized according to literature.[9]

Synthesis of 3[10]**:** A solution 2-decyltetradecan-1-ol (1eq, 5g, 14.1mmol), imidazole (1.5eq, 1.4g, 21.1mmol) and DCM (40ml) were cooled to 0°C under argon. Triphenylphosphine (1.2 eq, 4.4g, 16.9mmol) was dissolved followed by iodine (1.3eq, 4.6g, 18.3mmol). The mixture was warmed

to room temperature and stirred overnight. The reaction was quenched with a saturated solution of sodium sulfite until colorless (50ml) and the organic layer was washed 3 times with water, dried over magnesium sulfate, filtered, and the solvent was removed under reduced pressure. The resulting oil was purified via silica column chromatography (hexane) yielding a colorless oil (6.1g, 91%). ^{1}H NMR (400 MHz, $CDCl_3$) δ 1.29 (s, 46H), 3.29 (d, *J* = 4.5 Hz, 2H).

Synthesis of 4[11]**: 3** (1eq, 12.6mmol, 6g) was dissolved in THF (28mL) and degassed for 30 minutes. A 2M solution of allyl magnesium chloride (1.05eq, 13.2mmol, 7.8mL) was added dropwise and the reaction was refluxed at 70°C overnight. The reaction was quenched with 15mL water and 30mL 10wt% H_2SO_4 added very slowly dropwise and sequentially. The mixture was extracted 3 times with diethyl ether and washed with brine. The organic layer was dried over magnesium sulfate, filtered, and the solvent was removed under reduced pressure. The resulting oil was purified via silica column chromatography (hexane) yielding a colorless oil (4.2g, 90%). ^{1}H NMR (400 MHz, $CDCl_3$) δ 1.32 (s, 49H), 2.07 (m, 2H), 4.99 (m, 2H), 5.84 (m, 1H).

Synthesis of 5[12]: **4** (1eq, 11.32mmol, 4.3g) was dissolved in THF (30mL) and cooled to 0°C under argon. 9BBN (1eq, 11.32mmol, 22.65mL of 0.5M solution) was added dropwise and stirred at 0°C for 10 minutes. The solution was warmed to room temperature and heated at 60°C for 2 hours. The solution was cooled to 0°C and sodium hydroxide (2eq, 22.65mmol, 22.65mL of 1M solution) was added slowly followed by hydrogen peroxide (4eq, 45.31mmol, 5mL of 30wt% solution) dropwise. The reaction was then warmed to room temperature and heated to 60°C overnight. After cooling to room temperature, water was added to the reaction and it was extracted 3 times with diethyl ether. The organic layer was dried with magnesium sulfate, filtered and the solvent was removed under reduced pressure. The resulting oil was purified with silica column chromatography (hexane/EA, 8:2) yielding a colorless oil. (4.03g, 90%). ^{1}H NMR (400 MHz, $CDCl_3$) δ 1.28 (s, 53H), 3.67 (t, *J* = 6.6Hz, 2H).

Synthesis of 6: 6 was synthesized with a similar method to **3. 5** (1eq, 10.15mmol, 4g), Imidazole (1.5eq, 15.23mmol, 1.03g), DCM (30mL)triphenylphosphine (1.2eq, 12.19mmol, 3.19g), iodine (1.3eq, 13.2mmol, 3.35g), (3.8g, 74%) ^{1}H NMR (400 MHz, $CDCl_3$) δ 1.28 (s, 51H), 1.82 (m, 2H), 3.21 (t, J = 7.04, 2H).

Synthesis of 7[13]**:** THF (200mL) and sodium hydride (3eq, 240mmol, 9.6g 60% suspension in mineral oil) were cooled to 0°C. Triethylene glycol monomethyl ether (2eq, 160mmol, 26.2g) was added slowly and diallyl chloride (1eq, 80mmol, 10g) was added dropwise. The reaction was stirred at 0°C for 10 minutes, warmed to room temperature, and refluxed at 65°C overnight. The reaction was cooled to 0°C and quenched with 10mL water. The product was extracted with diethyl ether, washed with brine, and filtered. The solvent was removed under reduced pressure and a colorless oil was obtained (33.8g, 112%) **.** ^{1}H NMR (400 MHz, $CDCl_3$) δ 3.37 (s, 6H), 3.55-3.65 (m, 24H), 4.01 (s, 4H), 5.17 (s, 2H).

Synthesis of 8: 7 (1eq, 11.3mmol, 4.3g) and THF (30mL) were cooled to 0°C and 9BBN (1eq, 11.3mmol, 23mL of 0.5M solution) was added dropwise. The reaction was stirred for 10 minutes, warmed to room temperature, and heated to 60°C for 2 hours. Sodium hydroxide (2eq,

22.6mmol, 23mL of 1M solution) and hydrogen peroxide (4eq, 45.2mmol, 5mL of 30wt% solution) were added dropwise at 0°C, and the reaction was heated to 60°C overnight. After cooling, 60mL of water was added and the product was extracted with DCM and washed with brine. The organic layer was dried over magnesium sulfate, filtered, and the solvent was removed over reduced pressure. The resulting oil was used without further purification (3.1g, 72%) ^{1}H NMR (400 MHz, $CDCl_3$) δ 2.07 (m, 1H), 3.33 (s, 6H), 3.50-3.60 (m, 28H), 3.68 (d, *J*=5.01, 2H).

Synthesis of 9[14]**:** Sodium hydroxide (3eq, 37.6mmol, 1.5g) was dissolved in water (10mL) and added dropwise to a solution of **8** (1eq, 12.55mmol, 5g) and THF (10mL) at 0°C and the solution was stirred for 2 hours, allowing to warm to room temperature. 4-toluenesulfonyl chloride (1.5eq, 18.8mmol, 3.58g) was dissolved in THF (15mL) and added dropwise at 0°C and stirred at room temperature overnight. Water was added, and the product was extracted with DCM. The organic layer was dried with magnesium sulfate, filtered, and the solvent was removed under reduced pressure. The resulting oil was used without further purification (4.5g, 83%) ^{1}H NMR (400 MHz, $CDCl_3$) δ 2.25 (m, 1H), 3.38 (s, 6H), 3.34-3.66 (m, 28H), 4.13 (m, 2H), 7.35 (d, *J*=8.07, 2H), 7.79 (t, *J*=4.03, 2H).

Synthesis of 10[15] **(a-IID):** 6,6-dibromoisoindigo (1eq, 2.38mmol, 1g) and potassium carbonate (3eq, 7.14mmol, 0.987g) were heated to 110°C in DMF (60mL) for 45 minutes. **6** was added slowly and the reaction was refluxed at 100°C for 24 hours. After cooling, DMF was removed under reduced pressure and the product was dissolved in chloroform. The organic layer was washed with water and brine, then dried over magnesium sulfate, filtered, and the solvent was removed under reduced pressure. The product was purified by silica column chromatography (hexane/$CHCl_3$, 5:1) and recrystallized from hexane twice yielding a red solid (1.85g, 66%).

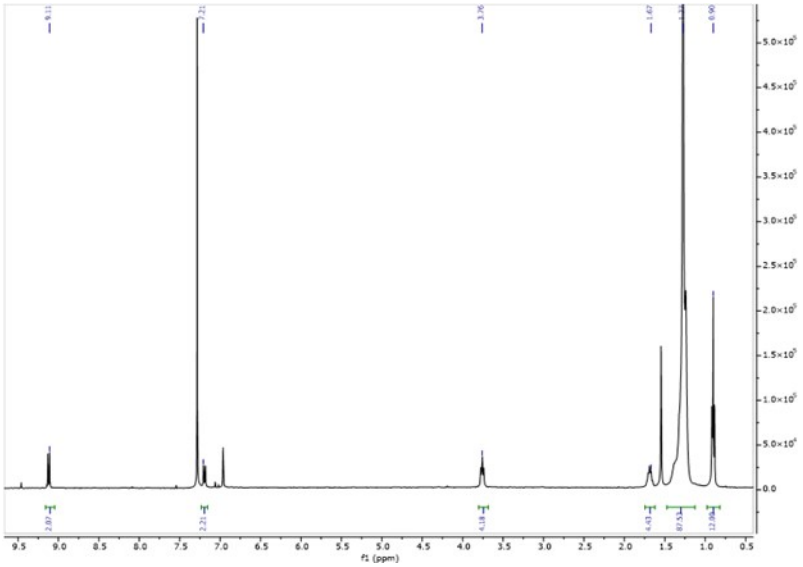

^{1}H NMR (400 MHz, $CDCl_3$) δ 0.90 (t, 12H) 1.27 (s, 90H), 1.69 (t, 4H), 3.76(t, 4H), 7.19 (dd, *J* = 8.6, 1.9Hz, 2H), 9.11 (d, *J* = 4.9Hz, 2H).

Synthesis of 11[15] **(g-IID):** 6,6-dibromoisoindigo (1eq, 1.78mmol, 0.75g), **9** (2.4eq, 4.28mmol, 2.36g) potassium carbonate (3eq, 7.14mmol, 0.740g), tetrabutylammonium bromide (0.5eq, 0.89mmol, 0.287g) were heated to 100°C in DMF (16mL) overnight. After cooling, DMF was removed under reduced pressure and the resulting liquid was purified by silica column chromatography (DCM/MeOH, 1%MeOH to 5%MeOH over 30min) yielding a dark red liquid (866mg, 41%).

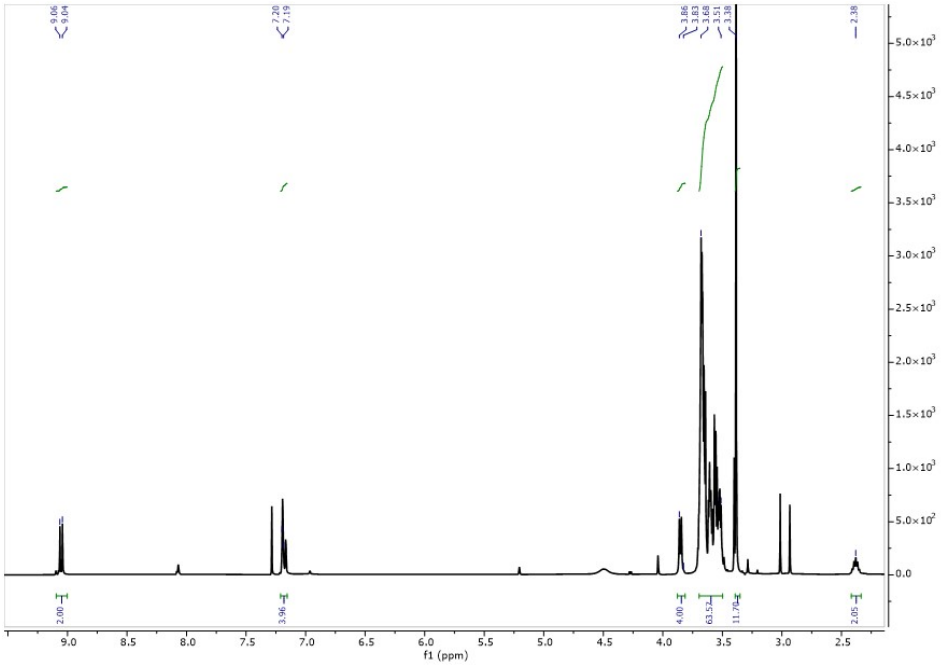

^{1}H NMR (400 MHz, $CDCl_3$) δ 2.37 (m, 2H), 3.38 (s, 12H), 3.67-3.35 (m, 56H), 3.85 (d, *J*=8.44, 4H), 7.17 (d, 3.99, 4H), 9.0 (d, *J*=8.45, 2H).

3. Polymer Synthesis

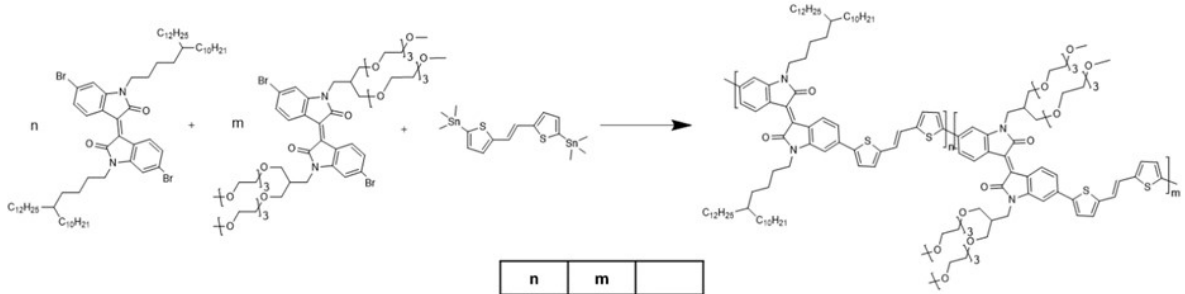

n	m	
1	0	**0g**
0.75	0.25	**25g**
0.50	0.50	**50g**
0.25	0.75	**75g***
0	1	**100g**

Scheme S2. Polymerization Conditions: x) Pd2(dba)3, P(o-tol)3, 135°C.

Synthesis of 0g: 10 (1eq, 0.2mmol, 286mg), **2** (1eq, 0.2mmol, 103.8mg), $Pd_2(dba)_3$ (0.04eq, 0.008mmol, 7.34mg), and P(*o*-tol)$_3$ (0.32eq, 0.064mmol, 19.52mg) were added to a Schlenk flask under argon. 6mL anhydrous chlorobenzene was degassed and added and the flask was sealed and heated at 135°C for 48 hours. After cooling, the solution was diluted with minimal chloroform and precipitated in cold methanol. The precipitate was collected by filtration and purified via Soxhlet extraction with methanol, acetone, hexane, and collected in chloroform. The chloroform solution was concentrated and precipitated in cold methanol. The final polymer was collected by filtration yielding a dark red solid.

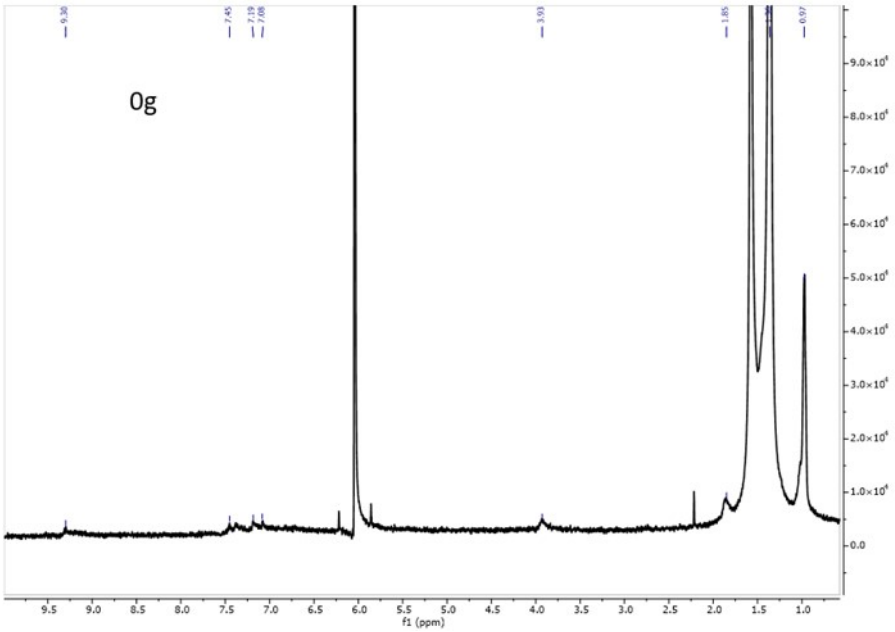

^{1}H NMR (500 MHz, TCE-d_2, 80°C) δ 0.97 (s), 1.36 (s), 1.85 (m), 3.93 (m), 7.08-7.19 (m), 7.45 (m), 9.30 (m).

Synthesis of 25g: **10** (0.75eq, 0.152mmol, 178.6mg), **2** (1eq, 0.202mmol, 105mg), $Pd_2(dba)_3$ (0.04eq, 0.008mmol, 7.42mg), and P(*o*-tol)$_3$ (0.32eq, 0.065mmol, 19.74) were added to a Schlenk flask under argon. **11** (0.25eq, 0.05mmol, 59.8mg) was dissolved in 7mL of chlorobenzene, degassed, and added to the flask which was then sealed and heated at 135°C for 48 hours. After cooling, the solution was diluted with minimal chloroform and precipitated in cold methanol. The precipitate was collected by filtration and purified via Soxhlet extraction with methanol, acetone, hexane, and collected in chloroform. The chloroform solution was concentrated and precipitated in cold methanol. The final polymer was collected by filtration yielding a dark red solid. The ratio of each monomer incorporated into the polymer was confirmed by comparing the ^{1}H NMR peaks of the side chain end methyl groups (alkyl – 0.97ppm, glycol – 3.4ppm).

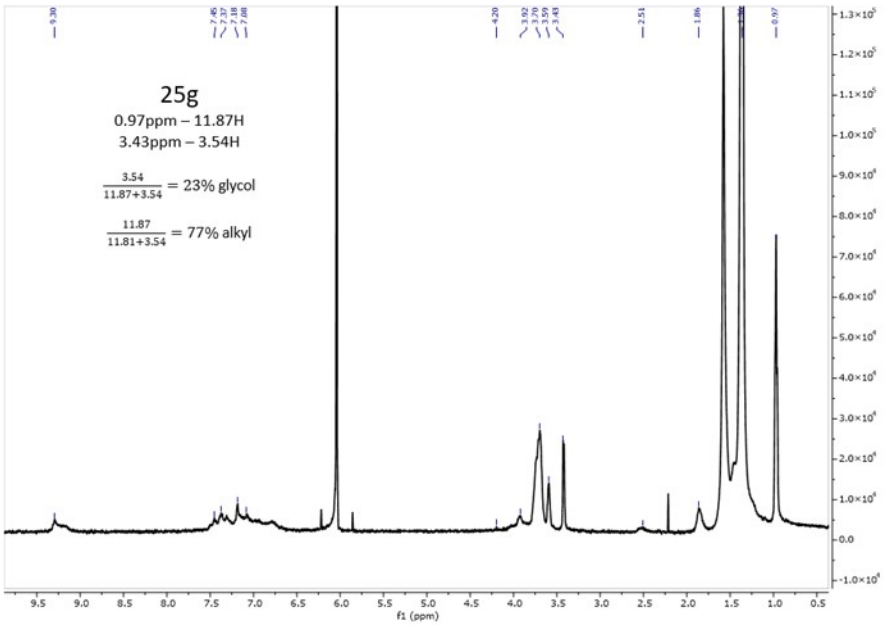

^{1}H NMR (500 MHz, TCE-d_2, 80°C) δ 0.97 (s), 1.36 (s), 1.86 (m), 2.51 (m), 3.43 (s), 3.59-3.7 (m), 3.92 (m), 4.20 (m), 7.08-7.19 (m), 7.37-7.45 (m), 9.30 (m).

Synthesis of 50g: Similar to **25g. 10** (0.50eq, 0.101mmol, 119.1mg), **2** (1eq, 0.202mmol, 105mg), $Pd_2(dba)_3$ (0.04eq, 0.008mmol, 7.42mg), and P(*o*-tol)$_3$ (0.32eq, 0.065mmol, 19.74), **11** (0.50eq, 0.101mmol, 119.7mg).

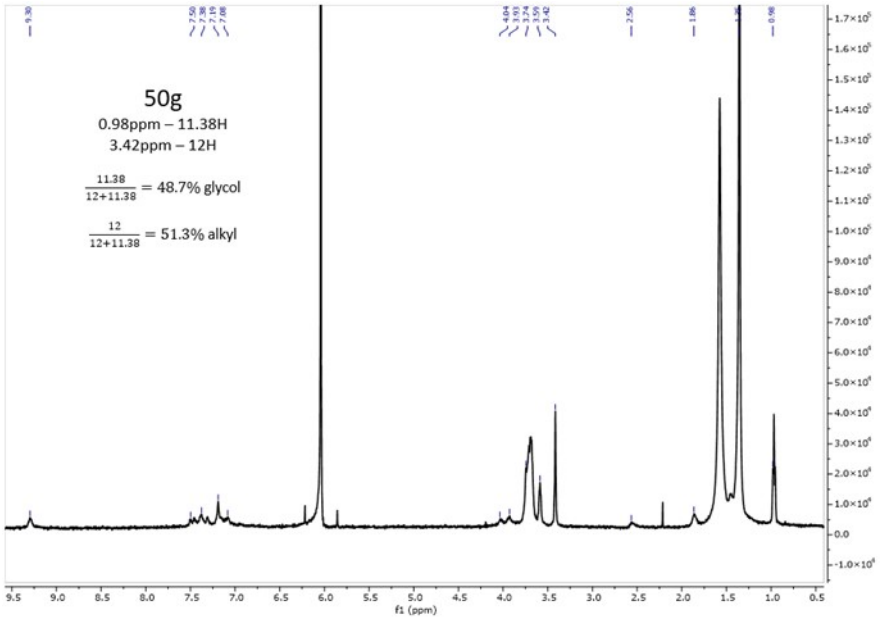

^{1}H NMR (500 MHz, TCE-d_2, 80°C) δ 0.98 (s), 1.36 (s), 1.86 (m), 2.56 (m), 3.42 (s), 3.59-3.92 (m), 7.08-7.19 (m), 7.37-7.45 (m), 9.30 (m).

Synthesis of 75g*: Similar to **25g. 10** (0.25eq, 0.05mmol, 59.6mg), **2** (1eq, 0.202mmol, 105mg), $Pd_2(dba)_3$ (0.04eq, 0.008mmol, 7.42mg), and P(*o*-tol)$_3$ (0.32eq, 0.065mmol, 19.74), **11** (0.75eq, 0.152mmol, 179.6mg).

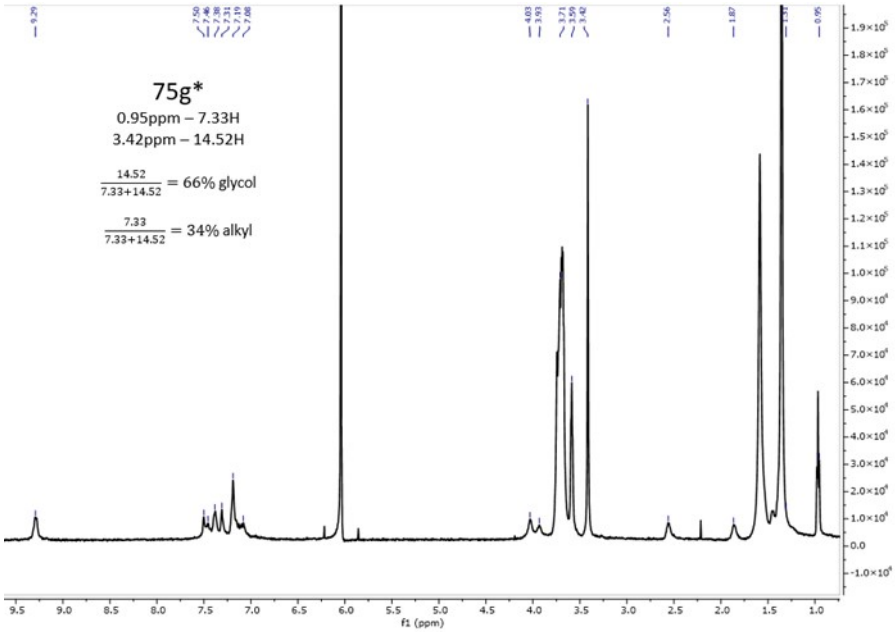

^{1}H NMR (500 MHz, TCE-d_2, 80°C) δ 0.95 (s), 1.31 (s), 1.87 (m), 2.5 (m) 3.42 (s), 3.59-371 (m), 3.93 (m), 4.03 (m) 7.08-7.19 (m), 7.38-7.50 (m), 9.29 (m).

Synthesis of 100g: Similar to **0g**. **2** (1eq, 0.202mmol, 105mg), $Pd_2(dba)_3$ (0.04eq, 0.008mmol, 7.42mg), and P(*o*-tol)$_3$ (0.32eq, 0.065mmol, 19.74), **11** (1eq, 0.2mmol, 237mg)

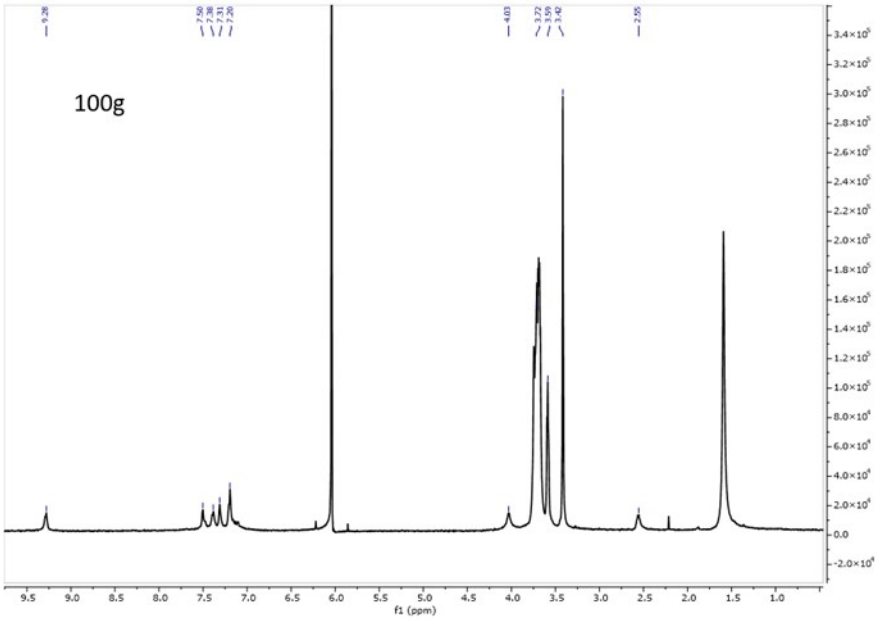

^{1}H NMR (500 MHz, TCE-d_2, 80°C) δ 2.55 (m), 3.42 (s), 3.59-372 (m), 4.03 (m), 7.20-7.50 (m), 9.28 (m).

4. Molecular Weight determination

Molecular weight and polydispersity data were collected on a TOSOH Bioscience EcoSEC HLC-8321 using 1,2,4-tricholorbenzene (TCB) at 150°C as the mobile phase at a flow rate of

1.0mL/min. The measured values for the polymers (in table below) containing glycol side chains were much lower than expected, and some smaller than the monomer molecular weights.

Table S1. Polymer molecular weight obtained from HT-GPC

Polymer	M_n (Da)	M_w (Da)	PDI
0g	65,574	120,136	1.83
25g	1,335	1,964	1.47
50g	1,017	2,416	2.37
75g*	933	2,878	3.08
100g	1,096	10,372	9.46

The low values are likely due to solubility issues in TCB of the more hydrophilic polymers as mentioned by Hu et al[17]. Using similar methods, DOSY NMR was used as an alternative to measure molecular weight based on diffusion coefficients.[17,18] A calibration curve was constructed using polystyrene standards of 3.35-65kDa. The aromatic peak of the DOSY spectra was used to determine the diffusion coefficient. A log-log plot was used to create a relationship between the known molecular weight and measured diffusion coefficient. The same parameters were then used to carry out DOSY experiments with the synthesized polymers. The backbone peak integrations were used to determine the average diffusion coefficients for consistency, however it is worth noting that side chain peaks gave different predicted molecular weights, higher than the backbone peaks. The estimated molecular weights using the polystyrene standard calibration curve are shown in the table below. Due to limit solubility in chloroform, the molecular weight of **0g-IID** was not determined using DOSY.

Table S2. DOSY parameters and estimated molecular weights

Polymer	DOSY Peaks used	Ave D (cm^2/s)	Log(D)	Log(M)	M (kDa)
100g	**Backbone**	**1.14742E-06**	**-5.94028**	**1.532497**	**34.07983**
	Glycol side chain	9.82875E-07	-6.0075	1.681359	48.01304
75g*	**Backbone**	**1.35743E-06**	**-5.86728**	**1.370867**	**23.48915**
	Glycol side chain	1.19696E-06	-5.92192	1.491851	31.03495
	Alkyl side chain	1.16154E-06	-5.93497	1.520743	33.1698
50g	**Backbone**	**1.66853E-06**	**-5.77767**	**1.17242**	**14.87375**
	Glycol side chain	1.11065E-06	-5.95442	1.563823	36.62886
	Alkyl side chain	1.03591E-06	-5.98468	1.630822	42.7388
25g	**Backbone**	**1.15361E-06**	**-5.93794**	**1.527324**	**33.67624**
	Glycol side chain	8.5826E-07	-6.06638	1.811739	64.82447
	Alkyl side chain	6.62805E-07	-6.17861	2.060262	114.8847

5. Material Characterization

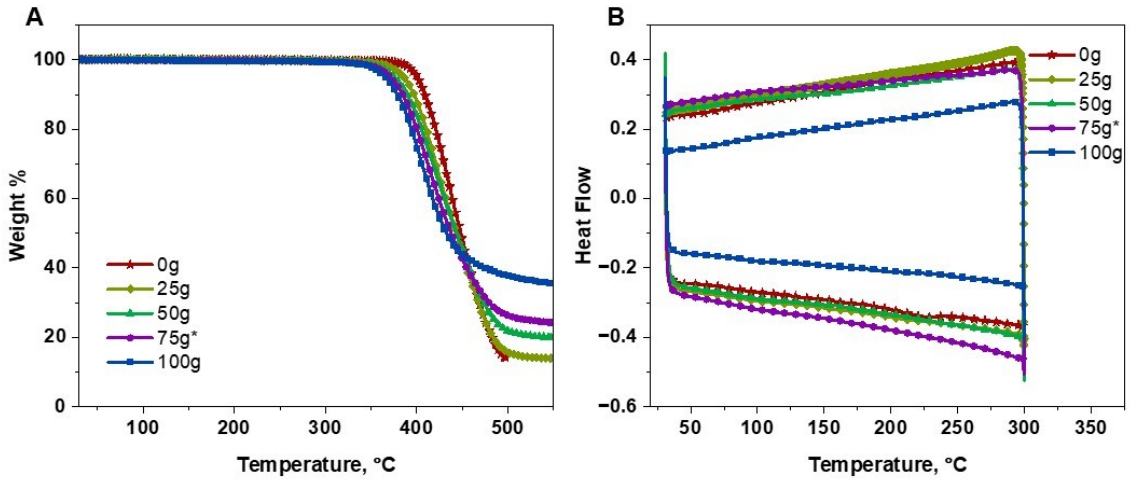

Figure S1. Thermal characterization of ***mg*-IID** polymers: A) TGA and B) DSC thermograms of the IID series.

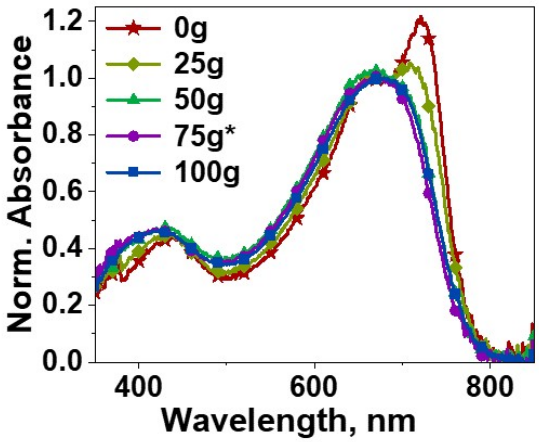

Figure S2. UV-vis absorbance of ***mg*-IID** polymers in chloroform.

6. Computational Simulations of HOMO and LUMO

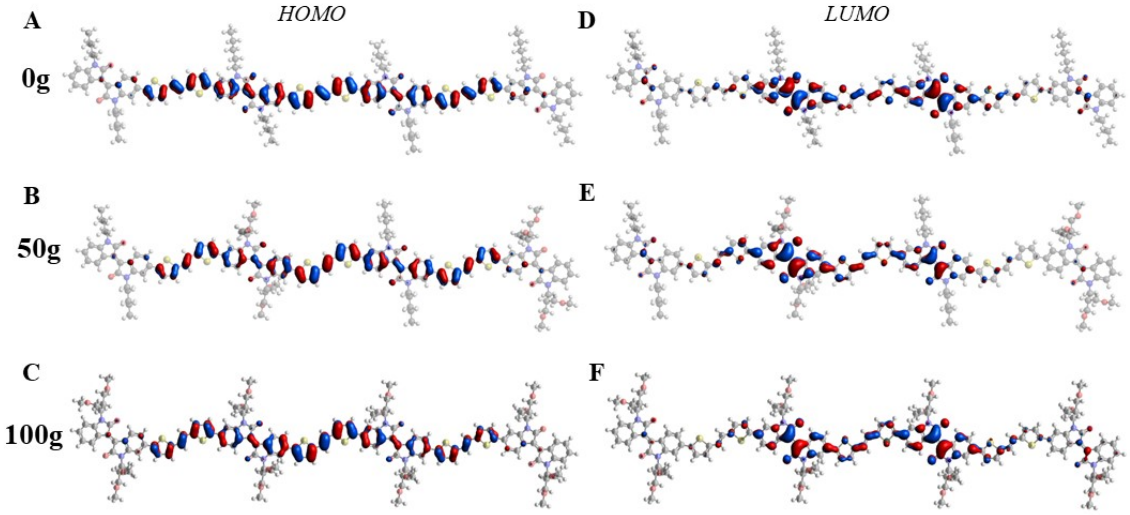

Figure S3. DFT simulations of HOMO (A-C) and LUMO (D-F) for **0g** (top), **50g** (middle), and **100g** (bottom).

7. AFM

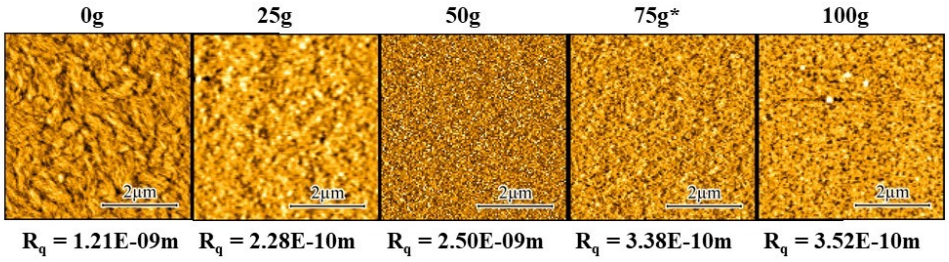

Figure S4. AFM height images of ***m*g-IID** films.

8. Contact Angle and Surface Energy

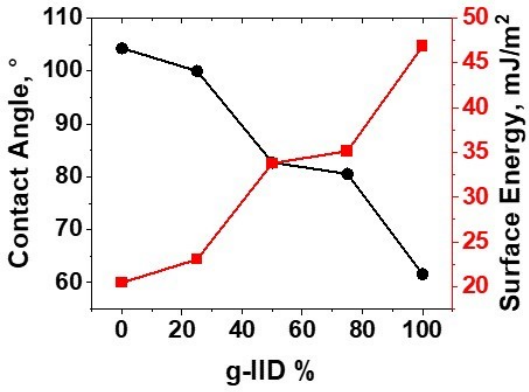

Figure S5. Contact angle and surface energy measurements of ***m*g-IID** films.

9. GIWAXs Parameters

Table S3. GIWAXs spacing parameters

Direction	In-plane		Out-of-plane	
	π-π stacking cell axis (010)		*d*-*d* stacking cell axis (100)	
	q (Å^{-1})	*d*-spacing (Å)	*q* (Å^{-1})	*d*-spacing (Å)
IID-TVT 100/0	1.75	3.58	0.251	25.041
IID-TVT 75/25	1.75	3.58	0.259	24.252
IID-TVT 50/50	1.76	3.56	0.267	23.505
IID-TVT 34/66	1.76	3.56	0.285	22.015
IID-TVT 0/100	NA	NA	NA	NA

Direction	In-plane		Out-of-plane	
	d-*d* stacking cell axis (100)		π-π stacking cell axis (010)	
	q (Å^{-1})	*d*-spacing (Å)	*q* (Å^{-1})	*d*-spacing (Å)
IID-TVT 100/0	NA	NA	NA	NA
IID-TVT 75/25	0.251	25.011	1.78	3.53
IID-TVT 50/50	0.263	23.916	1.78	3.53
IID-TVT 34/66	0.278	22.624	1.78	3.53
IID-TVT 0/100	0.311	20.203	1.77	3.55

10. DFT Configurations

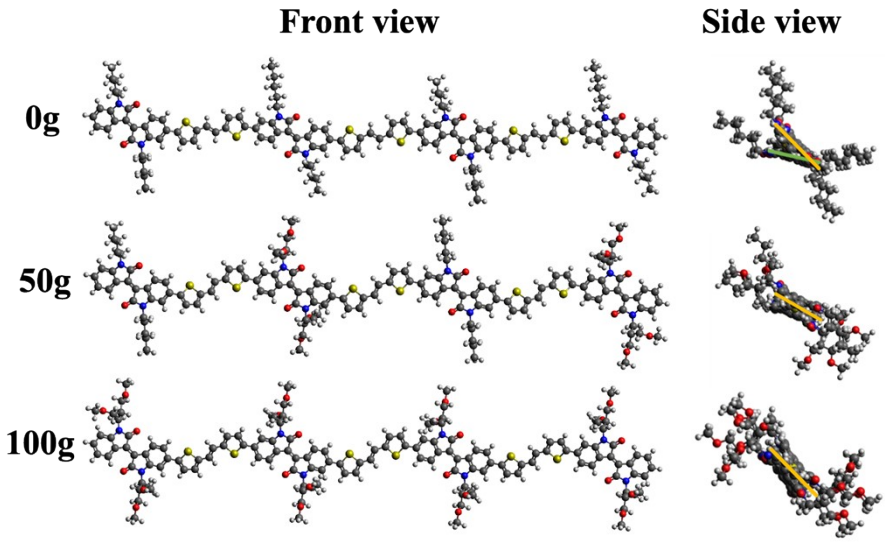

Figure S6. Density functional theory (DFT) calculations of polymer backbones. The yellow and green lines are added for visualization of chain planarity.

11. Electrochemical Performance

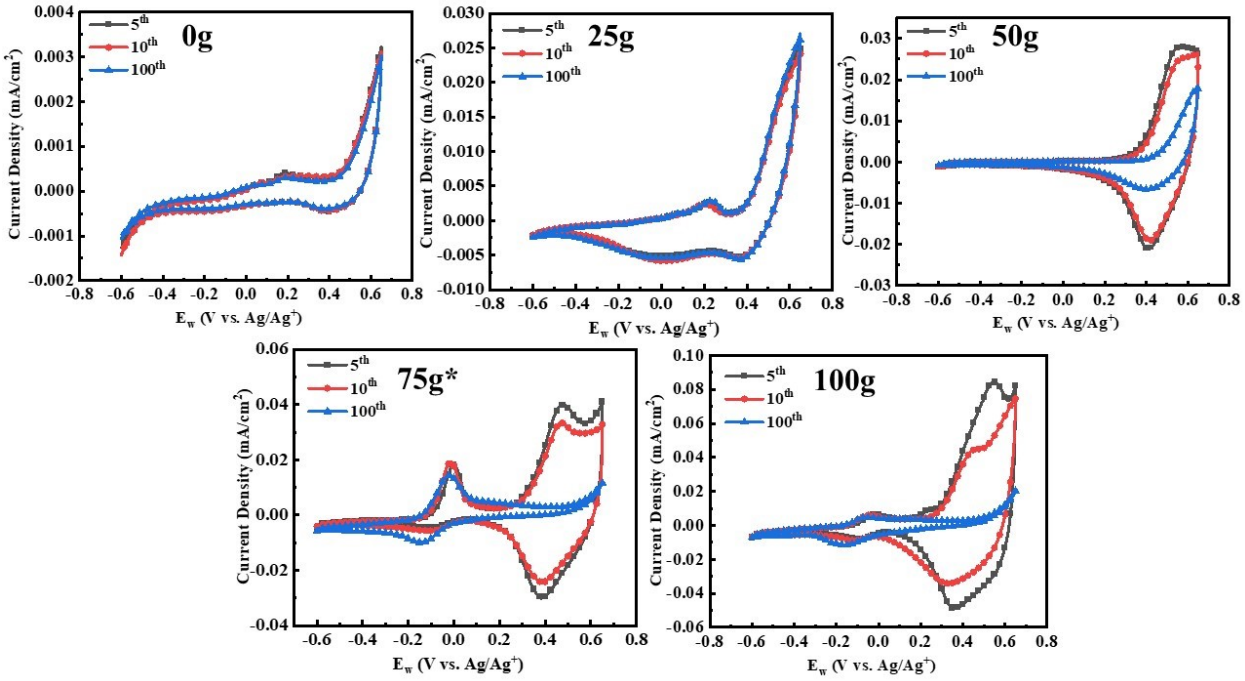

Figure S7. Cyclic voltammetry up to 100 cycles in 0.1M $LiPF_6$.

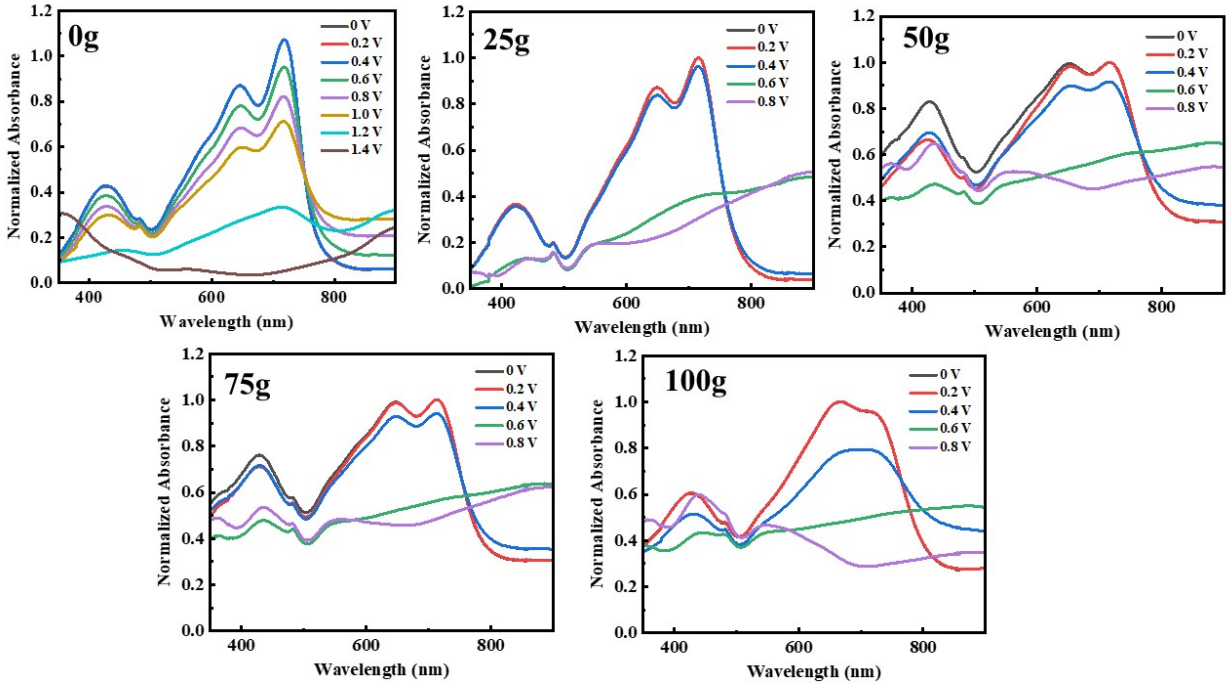

Figure S8. Normalized spectro-electrochemical spectra of ***m*g-IID** thin films with increasing amounts of glycol sidechains.

12. Electrochemical Impedance Spectroscopy

The data was fitted using the following equivalent circuit[19] and the ionic conductivity (σ_{ion} was calculated with the equation below, using the impedance at the chosen frequency as R_{ion}.

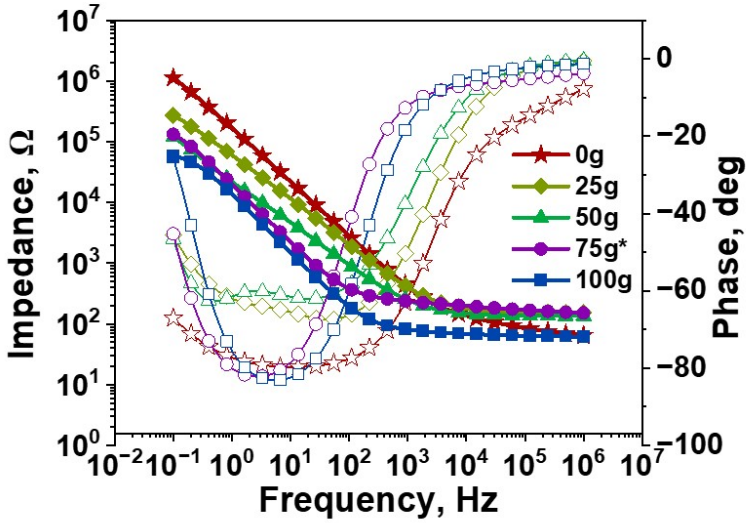

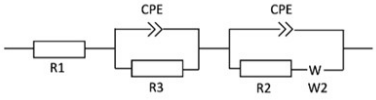

$$R_1 + \frac{Q_2}{R_2 + W_2} + \frac{Q_3}{R_3} \qquad \sigma_{ion} = \frac{1}{R_{ion}} \frac{l}{A}$$

At 1kHz	
R_{ion}, Ohms	σ_{ion}, S/cm
$3.77*10^{2}$	$1.73*10^{-8}$
$3.72*10^{2}$	$1.55*10^{-8}$
$2.35*10^{2}$	$8.60*10^{-9}$
$2.34*10^{2}$	$1.57*10^{-8}$
$7.94*10^{1}$	$4.22*10^{-8}$

Figure S9. Bode plot of ***m*g-IID** series in 0.1M $LiPF_6$ at -0.6V with equivalent circuit for data fitting and equation for calculating ionic conductivity.

13. OECT Performance

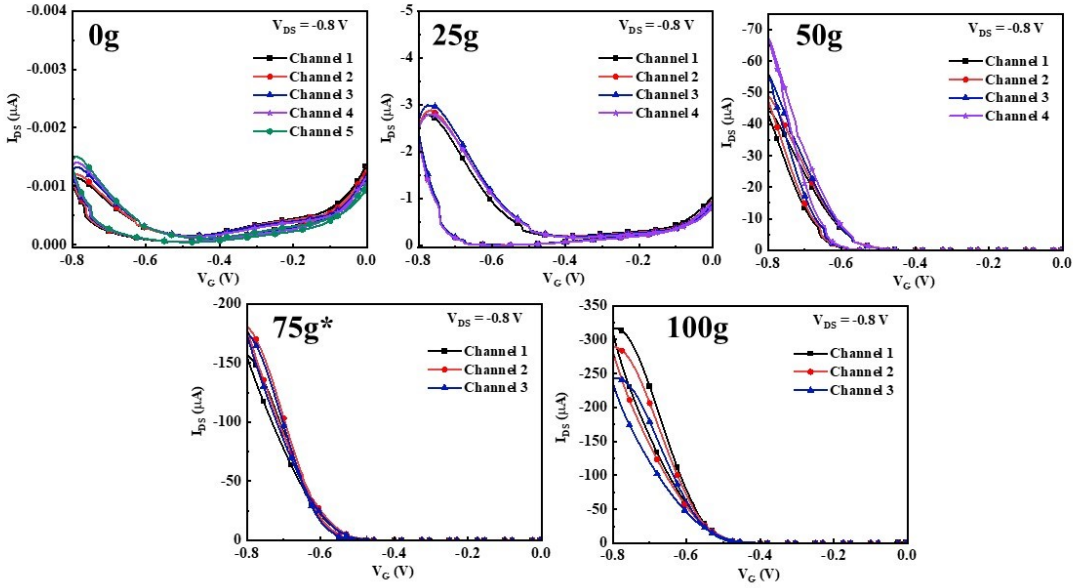

Figure S10. Characteristic transfer curves from ***m*g-IID** polymers in 0.1M $LiPF_6$ as the electrolyte.

Table S3. μC* of ***m*g-IID** polymers

Polymer	[a]C (F cm^{-2})	Thickness (nm)	[b]C* (F cm^{-3})	[c]μC* (F cm^{-1} V^{-1} s^{-1})	μ_{OECT} (cm^{-1} V^{-1} s^{-1})
0g	1.28E-05	58.5 (±2.88)	2.18	0.1008	0.0462
25g	1.37E-04	56.8 (±6.28)	24.14	0.2428	0.0100
50g	2.39E-04	20.1 (±0.98)	118.48	2.8898	0.0243
75g*	4.40E-04	29.3 (±4.01)	149.61	10.0773	0.0673
100g	8.29E-04	26.7 (±1.83)	309.44	12.2680	0.0396

[a]Capacitance calculated from CV measurement, [b]Capacitance divided by average film thickness, [c]extracted using the following equation: $g_m = \frac{W}{L} d\mu C^* (V_{Th} - V_G)$

References:

[1] M. J. Frisch, G. W. Trucks, H. B. Schlegel, G. E. Scuseria, M. A. Robb, J. R. Cheeseman, G. Scalmani, V. Barone, G. A. Petersson, H. Nakatsuji, X. Li, M. Caricato, A. V. Marenich, J. Bloino, B. G. Janesko, R. Gomperts, B. Mennucci, H. P. Hratchian, J. V. Ortiz, A. F. Izmaylov, J. L. Sonnenberg, D. Williams-Young, F. Ding, F. Lipparini, F. Egidi, J. Goings, A. Petrone, T. Henderson, D. Ranasinghe, V. G. Zakrzweski, J. Gao, N. Rega, G. Zheng, W. Liang, M. Hada, M. Ehara, K. Toyota, R. Fukuda, J. Hasegawa, M. Ishida, T. Nakajima, Y. Honda, O. Kitao, H. Nakai, T. Vrenven, K. Throssell, J. A. Montgomery Jr., J. E. Peralta, F. Ogliaro, M. J. Berapark, J. J. Heyd, E. N. Brothers, K. N. Kudin, V. N. Staroverov, T. A. Keith, R. Kobauashi, J. Normand, K. Raghavachari, A. P. Rendell, J. C. Burant, S. S. Iyengar, J. 2016, M. Cossi, J. M. Millam, M. Klene, C. Adamo, R. Cammi, J. W. Ochterski, R. L. Martin, K. Morokuma, O. Farkas, J. B. Foresman, D. J. Fox, **2016**.

[2] A. D. Becke, *J. Chem. Phys.* **1992**, *96*, 2155–2160.

[3] A. D. Becke, *Phys. Rev. A* **1988**, *38*, 3098–3100.

[4] W. J. Hehre, R. F. Stewart, J. A. Pople, *J. Chem. Phys.* **1969**, *51*, 2657–2664.

[5] A. K. Malde, L. Zuo, M. Breeze, M. Stroet, D. Poger, P. C. Nair, C. Oostenbrink, A. E. Mark, *J. Chem. Theory Comput.* **2011**, *7*, 4026–4037.

[6] A. P. Thompson, H. M. Aktulga, R. Berger, D. S. Bolintineanu, W. M. Brown, P. S. Crozier, P. J. in 't Veld, A. Kohlmeyer, S. G. Moore, T. D. Nguyen, R. Shan, M. J. Stevens, J. Tranchida, C. Trott, S. J. Plimpton, *Comput. Phys. Commun.* **2022**, *271*, 108171.

[7] A. I. Jewett, D. Stelter, J. Lambert, S. M. Saladi, O. M. Roscioni, M. Ricci, L. Autin, M. Maritan, S. M. Bashusqeh, T. Keyes, R. T. Dame, J.-E. Shea, G. J. Jensen, D. S. Goodsell, *J. Mol. Biol.* **2021**, *433*, 166841.

[8] T. Lei, Y. Cao, Y. Fan, C.-J. Liu, S.-C. Yuan, J. Pei, *J. Am. Chem. Soc.* **2011**, *133*, 6099–6101.

[9] X. Zhao, S. T. Chaudhry, J. Mei, in *Adv. Heterocycl. Chem.* (Eds.: E.F.V. Scriven, C.A. Ramsden), Academic Press, **2017**, pp. 133–171.

[10] M. Lee, M. J. Kim, S. Ro, S. Choi, S.-M. Jin, H. D. Nguyen, J. Yang, K.-K. Lee, D. U. Lim, E. Lee, M. S. Kang, J.-H. Choi, J. H. Cho, B. Kim, *ACS Appl. Mater. Interfaces* **2017**, *9*, 28817–28827.

[11] B. Fu, J. Baltazar, A. R. Sankar, P.-H. Chu, S. Zhang, D. M. Collard, E. Reichmanis, *Adv. Funct. Mater.* **2014**, *24*, 3734–3744.

[12] G.-J. N. Wang, F. Molina-Lopez, H. Zhang, J. Xu, H.-C. Wu, J. Lopez, L. Shaw, J. Mun, Q. Zhang, S. Wang, A. Ehrlich, Z. Bao, *Macromolecules* **2018**, *51*, 4976–4985.

[13] I.-S. Park, Y.-R. Yoon, M. Jung, K. Kim, S. Park, S. Shin, Y. Lim, M. Lee, *Chem. – Asian J.* **2011**, *6*, 452–458.

[14] J. Ge, L. Fan, K. Zhang, T. Ou, Y. Li, C. Zhang, C. Dong, S. Shuang, M. S. Wong, *Sens. Actuators B Chem.* **2018**, *262*, 913–921.

[15] Y. Wang, E. Zeglio, H. Liao, J. Xu, F. Liu, Z. Li, I. P. Maria, D. Mawad, A. Herland, I. McCulloch, W. Yue, *Chem. Mater.* **2019**, *31*, 9797–9806.

[16] H. Chen, Y. Guo, G. Yu, Y. Zhao, J. Zhang, D. Gao, H. Liu, Y. Liu, *Adv. Mater.* **2012**, *24*, 4618–4622.

[17] A. Hu, A. Nyayachavadi, M. Weires, G. Garg, S. Wang, S. Rondeau-Gagné, *RSC Appl. Polym.* **2023**, *1*, 292–303.

[18] P. Groves, *Polym. Chem.* **2017**, *8*, 6700–6708.
[19] M. Ahmed, D. T. Tran, J. Putziger, Z. Ke, A. Abtahi, Z. Wang, K. Chen, K. Lang, J. Mei, *ACS Macro Lett.* **2022**, *11*, 72–77.